Dynamics of Free, Damped, and Driven Oscillations

JINTIAN WANG, Exeter College, Oxford

February 11, 2026

Abstract

This experiment investigates the dynamics of free, damped, and driven simple harmonic motion using a rotational torsional oscillator. The system's natural frequency was measured experimentally as $\omega_0 = 4.42(3)$ rad s^{-1}, which agreed reasonably well with the theoretical value derived from the measured torsion constant κ and moment of inertia I. By varying the spacing of the eddy-current damping magnet (3, 4, and 6 mm), we observed that the Quality factor (Q) increased as the damping force decreased, consistent with theoretical expectations. Resonance curves obtained from the driven system demonstrated a clear amplitude peak near the natural frequency. However, the Q factors derived from driven oscillations were consistently lower than those from free decay, likely due to additional friction introduced by the driving mechanism.

1 Introduction

Simple harmonic motion (SHM) plays a fundamental role throughout physics. In an ideal simple harmonic oscillator, the restoring force acting on the system is directly proportional to the displacement from equilibrium and acts in the opposite direction, leading to periodic motion described by a second-order linear differential equation.

In realistic physical systems, however, oscillations cannot occur indefinitely without energy loss. Dissipative effects such as friction and air resistance introduce damping, causing the amplitude of oscillation to decrease over time. In addition, external forces may act on the oscillator and continuously supply energy to the system.

In this experiment, we investigate and verify the theoretical description of driven harmonic motion. Free oscillations, damped oscillations, and oscillations driven over a wide range of frequencies were studied experimentally. The effective spring constant, natural frequency, and damping constant of the oscillator were measured independently, allowing for quantitative comparisons between theoretical predictions and experimental results.

2 Theory

The apparatus consists of a disk of mass M and radius R coupled to a string-and-spring arrangement that provides an effective torsional spring constant κ. The equation of motion for the angular displacement $\theta(t)$ is given by Newton's second law for rotation:

$$I\ddot{\theta} + B\dot{\theta} + \kappa\theta = \tau_{\text{drive}}(t), \tag{1}$$

where $I = \frac{1}{2}MR^2$ is the moment of inertia, and B is the viscous damping coefficient. It is convenient to define

$$\gamma = \frac{B}{I},$$

so the linewidth parameter in the driven response is γ.

A static calibration of κ can be performed by applying a known torque $\tau = mgr$ (hanging mass m at pulley groove radius r) and measuring the angular deflection $\Delta\theta$:

$$\kappa = \frac{mgr}{\Delta\theta}. \tag{2}$$

For free, damped oscillations ($\tau_{\text{drive}} = 0$), the system oscillates at the damped frequency ω_γ:

$$\omega_\gamma = \omega_0\sqrt{1 - \frac{1}{4Q^2}} \quad \text{where} \quad \omega_0 = \sqrt{\frac{\kappa}{I}}. \tag{3}$$

The quality factor can be written as

$$Q = \frac{\omega_\gamma}{\gamma} \simeq \frac{\omega_0}{\gamma} \quad \text{(light damping)}. \tag{4}$$

In ringdown fits, PASCO commonly returns an envelope decay constant λ defined by $\theta_{\max}(t) \propto e^{-\lambda t}$. In this notation,

$$\lambda = \frac{\gamma}{2}, \qquad Q = \frac{\omega_\gamma}{\gamma} = \frac{\omega_\gamma}{2\lambda}.$$

For a system driven by a sinusoidal torque $\tau(t) = \tau_0\cos(\omega t)$, the steady-state amplitude is:

$$A(\omega) = \frac{\tau_0}{\kappa}\frac{\omega_0^2}{\sqrt{(\omega_0^2 - \omega^2)^2 + (\gamma\omega)^2}}. \tag{5}$$

The phase difference ϕ between the driver and the oscillator satisfies $\tan\phi = \gamma\omega/(\omega_0^2 - \omega^2)$.

3 Experimental Setup

In the experiment, we used a rotational oscillator consisting of a disk connected to a pulley and a string-and-spring restoring mechanism. A driving mechanism was used to apply a periodic torque to the disk, enabling us to study driven oscillations.

Eddy-current damping was produced by placing a magnet near the conducting disk; the damping strength was controlled by the magnet–disc spacing (3/4/6 mm).

We used the PASCO system to collect data. This system includes a rotary motion sensor that measures the angular displacement of the disk. The entire setup is mounted on a stable base to minimize external vibrations and ensure accurate measurements.

4 Data

4.1 Natural frequency

Placing one brass weight and a plastic hook on one side of the spring, and measure the displacement of the spring. Without any additional weights, the spring is stretched by 0.05 m. With one brass weight, the measured $\theta = -0.489(1)$ radians. Adding 20 grams on the left hand side of the spring, the measured $\theta = 1.769(1)$ radians. Adding 50 grams on the left hand side of the spring, the measured $\theta = 5.066(1)$ radians.

From measurements we also got the radius of the disk $R = 26.26(2)$ mm. Given that $g = 9.81\text{ms}^{-2}$, from Eq.2 we can calculate the torsion constant $\kappa = 2.413(6) \times 10^{-3}$ Nm rad^{-1}.

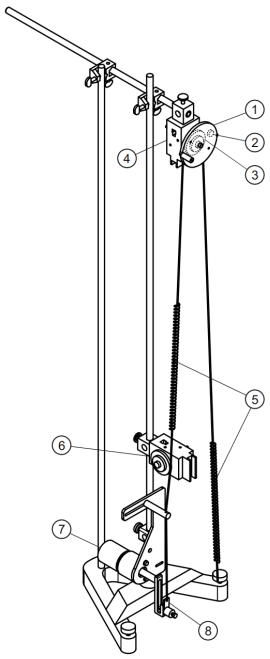

Figure 1: Experimental apparatus for studying driven harmonic motion (adapted from GP04 script [1]).

To measure the moment of inertia of the disk, we should get the radius and mass of the disk. The radius is $R = 47.66(2)$ mm and the mass is $M = 121.44(1)$ g, so we can calculate the moment of inertia of the disk $I = 1.379(1) \times 10^{-4}$ kg m^2.

Combine κ and I, we can calculate the theoretical value of the natural frequency of the system $\omega_0 = \sqrt{\kappa/I} = 4.18(1)$ rad s^{-1}. Therefore the theoretical period of the system is $T_0 = 2\pi/\omega_0 = 1.50(1)$ s.

Turning the disk to let it oscillate freely, we measured the period of oscillation as $T = 1.42(1)$ s, which yields $\boxed{\omega_0 = 4.42(3)\ \text{s}^{-1}}$. This value is slightly higher than the theoretical prediction. Since damping effects would theoretically *reduce* the observed frequency, this discrepancy is likely due to systematic uncertainties in the static measurement of the torsion constant κ or the moment of inertia I (e.g., assuming a uniform mass distribution for the disk), rather than frictional forces.

4.2 Damping system

Using the curve fitting tool in PASCO, we fit free oscillation data to extract the envelope decay constant λ and the oscillation frequency ω_γ. Taking three sets of data for each distance of the magnet from the disk, we calculate the quality factor using $Q = \omega_\gamma/(2\lambda)$. The results are shown below.

Distance	γ (s^{-1})	ω_γ (rad/s)	$\bar{Q}$
3 mm	0.460(3)	4.29(1)	4.66(6)
4 mm	0.422(3)	4.29(1)	5.09(7)
6 mm	0.242(2)	4.28(1)	8.9(3)

4.3 Forced oscillation

By applying a driving torque and measuring the amplitude as a function of driving frequency, we fit the data to Eq. 5 to extract γ and hence $Q = \omega_0/\gamma$ (driven steady-state method). The

results are shown below.

Distance	$\tau_0\omega_0^2/\kappa$ (rad^3/s^2)	ω_0 (rad/s)	γ (s^{-1})	$\bar{Q}$
3 mm	1.52(3)	4.895(7)	1.56(2)	3.13(5)
4 mm	1.49(2)	4.755(5)	1.06(1)	4.49(4)
6 mm	1.52(3)	4.604(5)	0.64(1)	7.2(1)

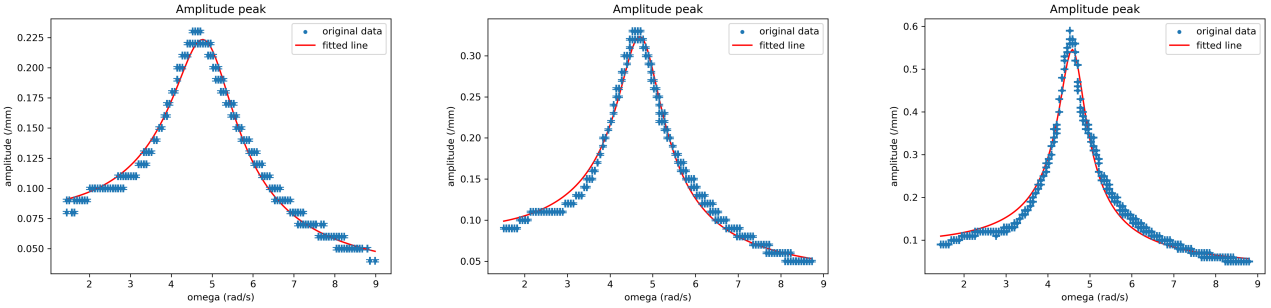

(a) 3 mm (b) 4 mm (c) 6 mm

Figure 2: Amplitude of oscillation as a function of driving frequency for different magnet–disc spacings. Points are measurements and solid curves are fits to Eq. 5.

4.4 Measuring the phase difference between the driven force and the oscillator

It is expected that when $\omega \ll \omega_0$, the phase difference $\phi \to 0$. Near the natural frequency ω_0, the phase difference $\phi \to \pi/2$. When $\omega \gg \omega_0$, the phase difference $\phi \to \pi$.

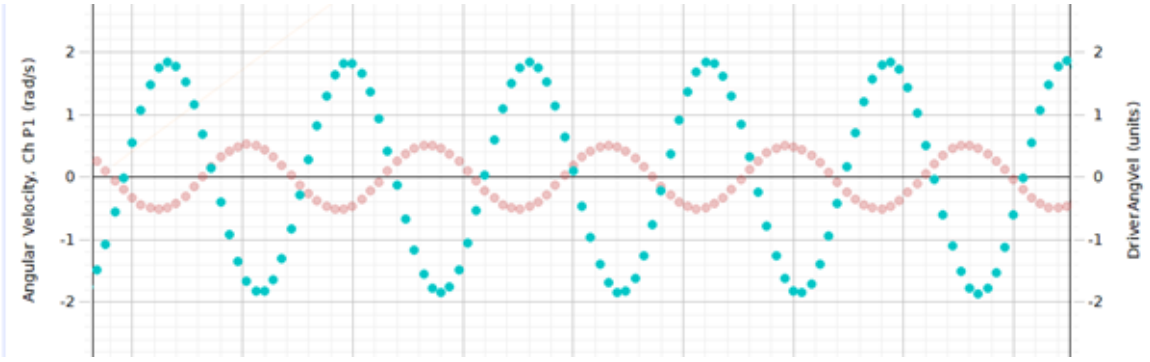

Figure 3: Oscillator and driver signals versus time at high driving frequency ($\omega \gg \omega_0$), showing an approximately π phase lag (anti-phase) at large ω.

5 Analysis

5.1 Analysing the data for damped oscillation

From the PASCO curve fitting tool, the data are consistent with exponential decay, as expected for a damped oscillator. We observe that as the distance of the magnet from the disk increases, the decay constant λ decreases and the quality factor Q increases. This is consistent with eddy current damping becoming weaker at larger magnet to disc separations.

The values of ω_γ (around 4.29 rad/s) are slightly lower than the measured free-oscillation frequency $\omega_{\text{free}} = 4.42(3)\ \text{rad}\,\text{s}^{-1}$, which is consistent with damping reducing the oscillation frequency. The small differences between ω_γ and ω_0 can be attributed to the damping effect, which slightly reduces the effective frequency of oscillation.

5.2 Analysing the data for driven oscillation

The resonance curves show that as the driving frequency approaches the natural frequency, the oscillation amplitude increases significantly and reaches a maximum near resonance. As the magnet is moved further away (reduced damping), the resonance peak becomes sharper and higher, indicating a higher Q, consistent with the free-decay method.

As the damping in the system decreases (as the magnet is moved further away), the width of the resonance peak narrows, and the maximum amplitude increases. This is because a higher Q factor corresponds to less energy loss per cycle, allowing the system to oscillate with larger amplitudes at resonance.

For the 6 mm spacing data, the resonance peak was observed at approximately $f_{\text{peak}} \approx 0.72\,\text{Hz}$. Using the measured free-oscillation angular frequency $\omega_{\text{free}} = 4.42(3)\ \text{rad}\,\text{s}^{-1}$, the corresponding frequency is $f_{\text{free}} = 0.703\,\text{Hz}$. The fractional difference is therefore 2.35%. This small difference is consistent with finite sweep effects and systematic uncertainties in identifying the peak frequency from discrete data.

As the driving frequency increases, the amplitude of oscillation decreases, which is expected. At low frequencies, the system can easily follow the driving force, resulting in larger amplitudes. However, as the driving frequency increases beyond the natural frequency, the inertia of the system prevents it from keeping up with the rapidly changing driving force, leading to a decrease in amplitude.

The Q factors obtained from the driven oscillation fits are generally lower than those obtained from the free-decay method. A plausible explanation is that the driven configuration introduces additional dissipation through the drive coupling (motor, linkage, string friction), increasing the effective damping and reducing the fitted Q.

6 Conclusion

In this experiment, we investigated the behavior of a driven harmonic oscillator and measured key parameters such as the natural frequency, damping coefficient, and Q factor. Our results showed that the natural frequency of the system was close to the theoretical value calculated from the torsion constant and moment of inertia. We also observed that as the distance of the magnet from the disk increased, the damping coefficient decreased and the Q factor increased, which is consistent with our understanding of damping in oscillatory systems. The amplitude of oscillation as a function of driving frequency exhibited a resonance peak near the natural frequency, and the width of the resonance peak was related to the damping in the system. The Q factors obtained from the driven oscillation data were generally lower than those obtained from the damped oscillation data, likely due to increased sensitivity to experimental uncertainties in the driven case. Overall, our findings are consistent with the theoretical predictions for driven harmonic motion, and the experiment provided valuable insights into the effects of damping and driving forces on oscillatory systems.

References

[1] GP04: Driven Harmonic Motion